J. Membrane Biol. 30, 319–350 (1977)


# Kinetic Characteristics of the Sulfate Self-Exchange in Human Red Blood Cells and Red Blood Cell Ghosts

K.F. Schnell, S. Gerhardt, and A. Schöppe-Fredenburg

Institute of Physiology, University of Regensburg, P.O.Box 397, D-8400 Regensburg, Germany

Received 29 October 1975; revised 21 June 1976

*Summary.* The sulfate and the chloride self-exchange fluxes were determined by measuring the rate of the tracer efflux from radioactively labeled human red blood cells and red blood cell ghosts. The concentration dependence and the pH-dependence of the sulfate self-exchange flux were studied. In addition, the effects of some monovalent and divalent anions on the sulfate and the chloride self-exchange fluxes were investigated.

The sulfate self-exchange fluxes saturate, exhibiting a concentration maximum at sulfate concentrations between 100 and 300 mM (25 °C). The position of the concentration maximum depends upon pH. At high sulfate concentrations a self-inhibition of the flux becomes apparent. The apparent half-saturation constant and the apparent self-inhibition constant at pH 7.2 were 30 mM and 400 mM respectively. Within the pH range of 6.3–8.5, both constants decreased with increasing pH. No saturation of the sulfate self-exchange flux was observed if the sulfate concentration was raised by substituting sulfate for isoosmotic amounts of a second salt (NaCl, $NaNO_3$, Na-acetate, Na-lactate, Na-succinate or $Na_2HPO_4$). Red blood cells and red blood cell ghosts display the same pattern of concentration responsiveness.

The sulfate self-exchange flux exhibits a pH-maximum at about pH 6.2 (37 °C). The location of the pH-maximum is little affected by variations of the sulfate concentration. The logarithmic plots (log $\vec{J}_{SO_4}$ *vs.* pH) revealed that the flux/pH relation can be approximated by two straight lines. The slopes of the alkaline branches of the flux/pH curves range from −0.55 to −0.86, the slopes of the acidic branches of the curves range from 0.08 to 1.14 and were strongly affected by changes of the sulfate concentrations. The apparent pK's obtained from the alkaline and from the acidic branches of the flux/pH curves were about 7.0 and 6.0, respectively. Intact red blood cells and red blood cell ghosts display the same type of pH-dependency of the sulfate self-exchange flux.

The sulfate self-exchange flux is competitively inhibited by nitrate, chloride, acetate, oxalate and phosphate. The chloride self-exchange flux is competitively inhibited by thiocyanate, nitrate, sulfate and phosphate. The inhibition constants for the various anion species increase in the given sequence.

The results of our studies indicate that the sulfate self-exchange flux is mediated by a "two-site transport mechanism" consisting either of a mobile carrier or a two-site pore. The experiments reported in this paper do not permit distinguishing between both transport mechanisms. The similarities of the sulfate and the chloride self-exchange flux and the mutual competition between sulfate and chloride point to a common transport system for both anion species.

A great number of experimental observations suggest that the anion transport across the red blood cell membrane is mediated by a specific transport system. The chloride and the sulfate permeabilities of the erythrocyte membrane are many orders of magnitude higher than that of unmodified black lipid membranes. The erythrocyte membrane displays a great anion permselectivity. The chloride self-exchange in human red cells is about five orders of magnitude faster than the sodium self-exchange, despite the fact that both ions are of comparable size (Wieth, 1972). The sulfate self-exchange is still about 100–1000 times faster than the sodium self-exchange. Other mammalian cells are almost completely impermeable to sulfate. Both the chloride (Cass & Dalmark, 1973; Gunn, Dalmark, Tosteson & Wieth, 1973; Dalmark, 1975) and the sulfate self-exchange flux (Schnell & Gerhardt, 1973; Gunn, Hartley & Horton, 1974) saturate and can be inhibited by amino group reagents (Passow & Schnell, 1969; Knauf & Rothstein, 1971; Poensgen & Passow, 1971; Cabantchik & Rothstein, 1972; Obaid, Rega & Garrahan, 1972) and by a large number of amphiphilic inhibitors (Passow & Schnell, 1969; Gunn & Tosteson, 1971; Dalmark & Wieth, 1972; Schnell, 1972; Gerhardt, Schöppe-Fredenburg & Schnell, 1973; Wieth, Dalmark, Gunn & Tosteson, 1973). The similarities between the sulfate and the chloride transport point to a common transport system for both anion species.

On the other hand, the detailed studies of the chloride and the sulfate transport have revealed some important differences between the sulfate and the chloride self-exchange. The chloride self-exchange flux is about 5 orders of magnitude greater than the sulfate self-exchange flux and the fluxes of both anion species exhibit different pH-profiles (Schnell, 1972; Gunn *et al.*, 1973; Wood & Passow, 1973; Dalmark, 1975). The chloride self-exchange flux seems to be mediated by an electrically silent transport mechanism (Scarpa, Cecchetto & Azzone, 1970; Hunter, 1971; Lassen, Pape & Vestergaard-Bogind, 1973; Tosteson, Gunn & Wieth, 1973), whereas a substantial fraction of the sulfate self-exchange takes place by ionic diffusion (Knauf & Fuhrmann, 1974; Passow, 1975, personal communication). SITS (4-acetamido-4′-isothiocyanostilbene-2,2′-disulfonic acid) and phlorhizin inhibit the self-exchange flux and the netflux of sulfate. Similarly, both the chloride self-exchange flux and the chloride netflux are inhibited by SITS, but phlorhizin has no inhibitory effect on the chloride netflux even if doses were applied which cause a 99% inhibition of the chloride self-exchange (Gerhardt & Schnell, 1975; Schnell & Gerhardt, 1975). These discrepancies could indicate basic

differences in the transport mechanisms of chloride and sulfate and the question is raised as to whether or not the transport system for both anion species is identical.

The present paper is concerned with the sulfate and the chloride transport across the erythrocyte membrane. The concentration dependence and the pH-dependence of the sulfate self-exchange flux under various conditions were studied. In addition, the effect of some monovalent and divalent anions on the sulfate and the chloride self-exchange was investigated. Attempts were made to graphically analyze the kinetic data by plotting procedures commonly used in enzymology. The results of our studies indicate that the sulfate self-exchange flux is governed by a two-site transport mechanism, either a cycling carrier or a two-site pore. The experimental data presented here do not permit us to distinguish between both transport mechanisms. The resemblence of the concentration response of the sulfate self-exchange with the chloride self-exchange and the mutual competition between both anion species give strong evidence towards the assumption that sulfate and chloride are transported by the same transport system.

## Materials and Methods

### *Calculations*

*Self-Exchange Flux.* The "self-exchange fluxes" of sulfate and chloride were determined from the sulfate and the chloride exchange at Donnan equilibrium. During a preincubation period, the erythrocytes were loaded with either radioactive sulfate or radioactive chloride. The red blood cells were then transferred into a nonradioactive solution of the same composition and the tracer back-exchange was measured. According to the theory of tracer exchange in a closed two-compartment system, the efflux of the radioactive isotope follows a single exponential equation (*cf.* Gardos, Hoffman & Passow, 1969):

$$y = y_\infty - (y_\infty - y_o)\, e^{-k_i t}, \tag{1}$$

$y$ is the radioactivity (cpm/ml) in the outside solution at time $t$, $y_o$ and $y_\infty$ denote the radioactivities in the outside solution at zero time and at infinite time, respectively; $k_i$ ($\text{min}^{-1}$) is the rate constant for the exchange of the anion species $i$, and $t$ (min) is the time. In order to calculate the self-exchange fluxes, the amounts of the respective anion species within the intracellular and the extracellular space have to be determined. The anion self-exchange flux $\vec{J}_i$ of the $i^{th}$ anion species is given by:

$$\vec{J}_i = k_i \frac{n_{\text{in}(i)} \cdot n_{\text{ex}(i)}}{n_{\text{in}(i)} + n_{\text{ex}(i)}}, \tag{2}$$

where $n_{\text{in}(i)}$ and $n_{\text{ex}(i)}$ (moles/ml suspension) are the amounts (referring to 1 ml of cell suspension) of the anion species $i$ in the intracellular and the extracellular space. At the limits of low cell concentrations, $n_{\text{in}(i)} \ll n_{\text{ex}(i)}$, and $y_\infty$ approaches the overall radioactivity

$\bar{y}$ within the suspension. Under these conditions, Eq. (1) reads:

$$y = \bar{y} - (\bar{y} - y_o)\, e^{-k_i t}. \tag{3}$$

Eq. (2) simplifies to:

$$\vec{J}_i = k_i \cdot n_{\text{in}(i)}. \tag{4}$$

The above simplification results in an overestimation of the exchange flux amounting to maximally 3% for a 10% (w/v) suspension and 1% for a 1% (w/v) cell suspension. Usually the error is even less. It is difficult to make an estimate of the overall error involved in the flux measurements. According to our experience, only changes of more than 10% can be considered as significant. Hence, the small error which is introduced by the above simplification can be ignored as compared to other sources of error.

The self-exchange fluxes as calculated by means of Eqs. (2) or (4) have the dimension moles $\times$ min$^{-1}$ $\times$ ml suspension. By knowing the concentration of the suspension ((%w/v), the fluxes can be expressed in moles $\times$ min$^{-1}$ $\times g$ cells$^{-1}$. The term "$g$ cells" refers to the wet weight of tightly packed red blood cells under standard conditions (10 min centrifugation at 5000 $\times$ g, pH 7.3, 20 °C). The dry weight of 1 g cells under the above conditions amounts to $0.353 \pm 0.003$ g (n = 141, average $\pm$ standard deviation). Therefore, the fluxes can be easily converted into moles $\times$ min$^{-1}$ $\times g$ cells dry weight$^{-1}$.

### *Execution of the Sulfate Self-Exchange Experiments*

*Materials.* The experiments were conducted with blood from healthy adult donors. The blood was withdrawn under sterile conditions and stored no longer than 4 days at 4 °C. Coagulation was prevented by adding an acid-citrate-dextrose solution. Before the experiments were begun, the red blood cells were washed three times in about 10 volumes of a 165 mM NaCl solution whereby plasma and buffy coat were removed. After the last washing, the cells were spun down for 10 min at 5000 $\times g$ (pH 7.3, 20 °C) and the supernatant was completely suctioned off. All fluxes were related to the wet weight of tightly packed red blood cells at the end of the washing procedure. Care was taken that no cells were lost during the further preparations. The chemicals employed were of GR grade. Amphotericin B was kindly supplied by Dr. Reinhard, v. Heyden-Chemie, Regensburg.

*Modification of the Sulfate Concentration, Titration and Labeling of the Red Blood Cells.* 4 $g$ of tightly packed red blood cells or ghosts made of 4 $g$ tightly packed red blood cells were added to 36 ml of incubation solution to make a 10% (w/v) suspension. The sulfate concentration of the incubation solution was varied in two fashions: (1) Sulfate was added in exchange for isoosmotic amounts of a second salt. For this purpose, a definite volume of $Na_2SO_4$-stock solution or the $K_2SO_4$-stock solution was replaced by the same volume of the respective stock solution of a second salt. The concentrations of the stock solutions were 264 mM with respect to $Na_2SO_4$, $K_2SO_4$, Na-succinate, $Na_2HPO_4$ and 330 mM with respect to NaCl, $NaNO_3$, Na-acetate and Na-lactate. During a preincubation period of 2 hrs (pH 7.2, 37 °C) the red blood cells or the red blood cell ghosts were labeled with $^{35}SO_4$. (2) Various amounts of either $Na_2SO_4$ or $K_2SO_4$ were added to a solution containing 23 mM K-phosphate buffer and 30 mM sucrose. The cells or the ghosts were equilibrated for 2 hrs at 37 °C. pH was adjusted by slowly adding either 0.1 n $H_2SO_4$ or 0.1 n KOH. After these 2 hrs the red blood cells or the red blood cell ghosts were transferred to a solution of the same composition and loaded with $^{35}SO_4$. The labeling of the cells took 45 min at 37 °C and was extended to 120 min at alkaline

pH. This time period is sufficiently long to reach a distribution of $^{35}SO_4$ which differs less than 5% from the ideal equilibrium distribution of sulfate. Knowing the rate constant $k_{SO_4}$ for the tracer back-exchange and the amount of intracellular sulfate $n_{in(SO_4)}$, the sulfate self-exchange flux $\vec{J}_{SO_4}$ was calculated by using Eq. (4).

*Determination of the Rate Constant of the $^{35}SO_4$ Back-Exchange.* The sulfate back-exchange at Donnan equilibrium was measured by transferring the radioactively labeled cells into a nonradioactive solution of the same composition. The cell concentration was 10% (w/v) if not indicated otherwise. The appearance of the radioactivity within the outside solution was measured by centrifuging the suspensions at suitable time intervals and measuring the radioactivity in the supernatant. In addition, duplicate samples were withdrawn from the suspension in order to determine the overall radioactivity. The samples were deproteinized with trichloracetic acid (final concentration: 7.5%), the precipitate was spun down, and the radioactivity was counted with a Packard Liquid Scintillation Spectrometer type 2425. For this purpose, 1 ml of the deproteinized supernatant was mixed with 10 ml of a triton X-100-toluene scintillation mixture (400 ml triton-X-100, 600 ml toluene, 5.5 *g* PPO and 0.1 *g* POPOP). The rate constants $k_{SO_4}$ for the tracer back-exchange were determined by fitting the cpm/time curves to Eq. (3) by means of a least squares fit procedure.

*The Determination of the Intracellular Sulfate.* For determination of intracellular sulfate, the cells or the red blood cell ghosts were incubated for 2 hr (37 °C) at acidic and neutral pH and up to 6 hr (37 °C) at alkaline pH. In order to test if an equilibrium distribution is reached, trial runs were made and the time course of the sulfate uptake was followed. The amount of intracellular sulfate $n_{in(SO_4)}$ was calculated from the cellular radioactivity and the specific activity of sulfate in the incubation solution at isotopic equilibrium.

The cellular radioactivity was determined as follows: at the end of the preincubation period, double samples of 2 ml each were withdrawn from the suspension, the cells were spun down and washed twice with 330 mM NaCl (0 °C). At 0 °C the cells are completely impermeable to sulfate, and the extracellular sulfate can be removed by washing the cells. Care was taken that no cells were lost during this washing procedure. Finally the cells were hemolyzed by adding 1.8 ml of distilled water and small amounts of saponin, and the hemolysate was deproteinized by adding 2 ml of a 15% trichloracetic acid (final concentration: 7.5%). The final volume of the hemolysate amounted to 4 ml. The radioactivity within the hemolysate was counted.

### *Chloride Back-Exchange Experiments*

*Preparation of the Red Blood Cells.* The chloride back-exchange experiments were conducted with amphotericin B treated red blood cells. A 10% cell suspension (w/v) was used. Chloride concentration and pH were adjusted to the required values (*cf.*: amphotericin B treatment of red blood cells). The cells were then incubated in solutions containing either 10 or 100 mM KCl, 25 mM K-phosphate buffer, and 30 mM sucrose, as well as varying concentrations of the inhibiting anion species. During a 60 min preincubation at 37 °C, the cells were equilibrated and loaded with $^{36}Cl$. At alkaline pH, the preincubation period was extended up to 2 hr if sulfate anions were present. After equilibration, the cells were cooled to 0 °C and centrifuged for 10 min at 5000 $\times g$. The supernatant was completely suctioned off. The remaining cells were aspirated into a 2 ml plastic syringe and stored for a short time at 0 °C. For the calculation of the chloride self-exchange flux Eq. (4) was used.

*Determination of the Rate Constant of the $^{36}Cl$ Back-Exchange.* The rate of the $^{36}Cl$ back-exchange was measured as follows: 40 ml of the back-exchange solution was placed

into a well stirred and thermostated chamber and the temperature was adjusted to 0 °C. The back-exchange solution had exactly the same composition as the solution during the equilibration period except that it contained no radioactive chloride. The tracer efflux was initiated by injecting 0.4 *g* of $^{36}$Cl-labeled cells into the back-exchange solution. Serial samples were removed from the suspension at suitable time intervals by using the filtration technique of Dalmark and Wieth (1970, 1972). The cell concentration during the $^{36}$Cl-back-exchange was 1% (w/v). For filtration, Swinnex 25 filter holders, Millipore prefilters (AP 2502500) and Sartorius filters (Sartorius 1303, pore size 1.2 μ) were used. In addition, duplicate samples of 2 ml each were withdrawn from the suspensions in order to determine the overall radioactivity. The red blood cells were hemolyzed by small amounts of saponin. The hemolysate and the cell-free solution as obtained by filtration were deproteinized with trichloracetic acid (final concentration 7.5%), and the radioactivity was counted as described above. The rate constant $k_{Cl}$ of the tracer back-exchange was obtained from the time course of the tracer exit by fitting the cpm/time curves to Eq. (3). For this purpose, a least squares fit procedure was employed.

*Determination of Intracellular Chloride.* The intracellular chloride $n_{in(Cl)}$ was calculated from the cellular radioactivity at equilibrium and the specific activity of chloride in the incubation solution at equilibrium. To determine the intracellular chloride, two methods were employed which gave the same results: (1) At the end of the equilibration period. 10 ml of the samples were withdrawn and the cells were spun down for 10 min at 5000 × *g*. Exactly 8 ml of the supernatant were withdrawn, the radioactivity was counted and the chloride concentration was determined by coulometric titration using a chloride titrator (Chlor-o-Counter, Marius, Utrecht). The remaining cells were resuspended, transferred into a thin nylon tube (70 mm long, 3 mm id), and centrifuged for 10 min at 40,000 × *g*. The supernatant was completely discarded and the nylon tubes were cut 2 mm below the sediment supernatant interface. The cells were collected in a centrifuge tube of larger volume and hemolyzed with distilled water and saponin. After deproteinization of the hemolysate with trichloracetic acid (final concentration: 7.5%), the cellular radioactivity was counted and the dry weight of the precipitate was measured. (2) The equilibrated red blood cells were washed twice in 165 mM Na-salicylate solution (0 °C, pH 7.2). After the last washing the cells were hemolyzed as described above, deproteinized and the cellular radioactivity was counted. The dry weight of the precipitate was again measured.

*Amphotericin B Treatment of Red Blood Cells.* In order to vary the anion concentration over a larger range, we made use of the dialysis technique of Cass and Dalmark (1973). Instead of nystatin the antibiotic amphotericin B was used, which at low concentrations (5 μg/ml) has little effect upon the sulfate and the chloride permeability but renders the cells leaky for potassium and sodium (*cf.* Results, Table 1). The titration procedure varies somewhat depending upon the sulfate and the chloride concentrations to be established. If the cells were incubated in isotonic or hypertonic solutions, the following procedure was applied: 4 *g* tightly packed red blood cells were incubated in 36 ml of a solution to make up a 10% (w/v) suspension. The incubation solution contained varying amounts of $K_2SO_4$ or KCl, 25 mM K-phosphate buffer, 30 mM sucrose and 5 μg/ml amphotericin B. The pH was adjusted by titrating the cells either with 0.1 N $H_2SO_4$ or 0.1 N HCL or 0.1 N KOH. The cells were incubated for 90 min at 37 °C and equilibrated. Then the cells were spun down, washed with a solution of the same composition, resuspended and loaded with either $^{35}SO_4$ or $^{36}$Cl. If the sulfate concentrations to be established were lower than 75 mM or if the chloride concentrations to be established were lower than 100 mM, the titration was started with a solution which initially contained either 75 mM $K_2SO_4$ or 100 mM KCl, 25 mM K-phosphate buffer, 30 mM sucrose and 5 μg/ml amphotericin B. After a break of about 20 min, hypotonic phosphate buffer-sucrose solution

(25 mM K-phosphate buffer and 30 mM sucrose) was slowly added until the final concentrations of sulfate and chloride were reached. pH was adjusted as described above. The titration usually took 120 min at 37 °C. After titration, the cells were again centrifuged and washed in their respective solutions. Thereafter they were resuspended and loaded either with $^{35}SO_4$ or $^{36}Cl$.

*Preparation of Erythrocyte Ghosts.* The red blood cell ghosts were prepared according to the method of Bodemann and Passow (1972) and Lepke and Passow (1972). The red blood cells were washed in an isotonic KCl solution (165 mM) as described above. 10 *g* of washed and tightly packed cells were added to 10 ml of a 165 mM KCl solution to give a 50% (w/v) cell suspension. Thereafter, the cells were hemolyzed for 5 min at 0 °C by adding 2 ml of the suspension to 20 ml of a hypotonic $MgSO_4$-acetic acid solution (4 mM $MgSO_4$, 3.5 mM acetic acid). Under these conditions, a pH of 6.2 is spontaneously established. In order to restore isotonicity, 2 ml of a hypertonic KCl-Tris-solution were added to the hemolysate (1.99 M KCl+20 mM Tris-hydroxymethyl-aminomethane) and the cells were kept at 0 °C for another 10 min. Usually, the pH shifts to 7.2. If the required pH was not spontaneously reached, the cells were titrated by adding small amounts of either acetic acid or Tris. Subsequently, the temperature was raised to 37 °C and the incubation was continued for 45 min. During the resealing period, 90% of the cells regain their original cation and anion permeability. The ghosts still contain about 5% of the hemoglobin of intact red blood cells. After resealing, the ghosts were washed twice in about 10 volumes of isotonic KCl solution. All experiments were run with the crude ghost population. No attempts were made to separate leaky cells and resealed ghosts by density gradient centrifugation. In order to make the flux measurements comparable to one another, the fluxes were related to the wet weight of fresh cells used for the preparation of ghosts.

## Results

### *The Concentration Dependence of the Sulfate Self-Exchange Flux*

Previous studies have shown that under suitable conditions the chloride (Cass & Dalmark, 1973; Gunn *et al.*, 1973; Dalmark, 1975) and the sulfate self-exchange flux (Schnell & Gerhardt, 1973; Gunn *et al.*, 1974) saturate. No saturation of the sulfate or the chloride flux was observed if the sulfate or the chloride concentrations were raised in exchange for isoosmotic amounts of a second salt (Lepke & Passow, 1971; Dalmark, 1972; Gunn *et al.*, 1973). The results of our studies are presented here in detail.

Fig. 1 displays the effect of the sulfate concentration upon the sulfate self-exchange flux. The flux is plotted *vs.* the extracellular sulfate concentration. The experiments were conducted in different incubation solutions. Sulfate was substituted for isoosmotic amounts of a second salt. In order to cover a larger concentration range, double isotonic solutions were employed. Although the sulfate concentration was raised to 264 mM, no saturation of the sulfate self-exchange flux was reached. In chloride, nitrate, or acetate solutions, the graphs show an overlinear increase of

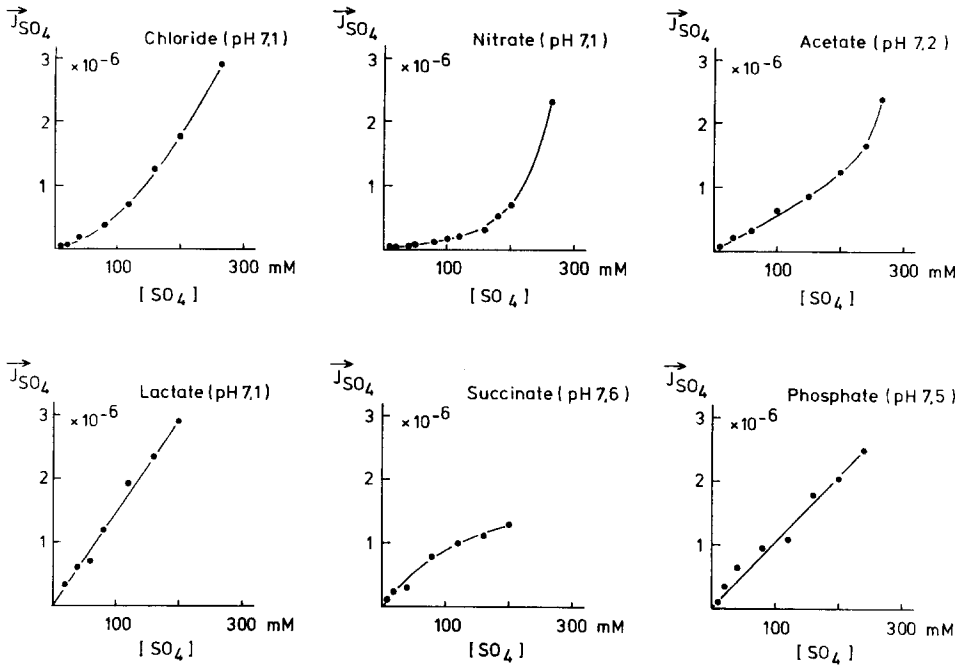


Fig. 1. Concentration dependence of the sulfate self-exchange flux in red blood cells. Ordinate: Sulfate self-exchange flux $\vec{J}_{SO_4}$ (moles × min$^{-1}$ × g cells$^{-1}$). *Abscissa:* Extracellular sulfate concentration [$SO_4$] (mM). Concentration of the stock solutions (in mM). 264 $Na_2SO_4$, 330 NaCl, 330 $NaNO_3$, 330 Na-acetate, 330 Na-lactate, 264 Na-phosphate buffer, 264 Na-succinate. The sulfate concentration of the incubation solution was increased by substituting a definitive volume of the $Na_2SO_4$ stock solution for the same volume of the stock solution of another salt. pH as indicated in the figure. Cell concentration: 10% (w/v), 37 °C

the sulfate flux with increasing sulfate concentration. A nearly linear relation between sulfate flux and sulfate concentration was found in lactate and phosphate media. In succinate solutions, the flux curves exhibit a tendency to saturate without reaching a plateau.

Experiments of the same type were conducted with red blood cell ghosts. After resealing, the ghosts were incubated in $KCl/K_2SO_4$ solutions of different composition, loaded either with radioactive chloride or sulfate, and the self-exchange fluxes were measured. The results are shown in Fig. 2. The concentration response of the sulfate self-exchange flux closely resembles that of intact red blood cells. The sulfate self-exchange flux increases overlinearly as the sulfate concentration is raised. Likewise, the chloride self-exchange flux did not saturate but increased almost linearly up to chloride concentrations of 330 mM.

In a second series of experiments, the concentration dependence of the sulfate self-exchange was measured without maintaining tonicity. Red

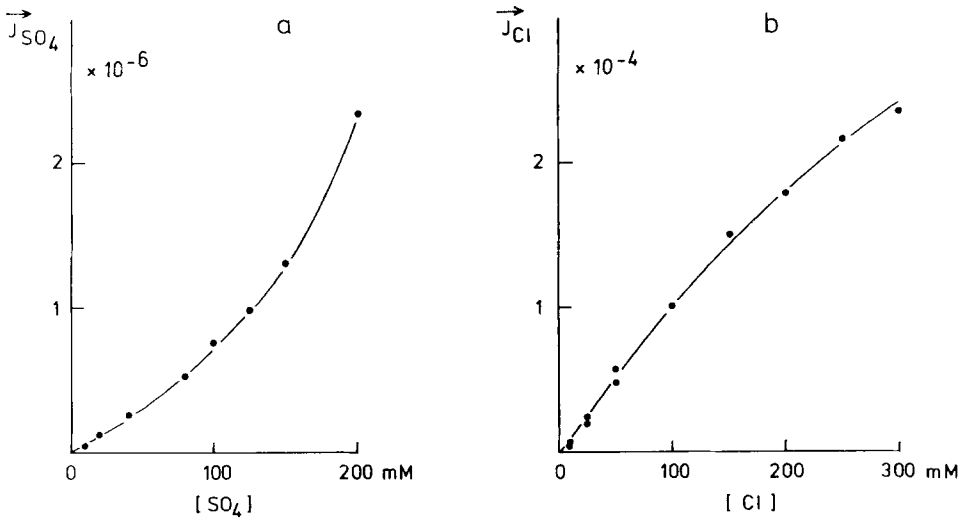


Fig. 2. Concentration dependence of the sulfate and the chloride self-exchange fluxes in red blood cell ghosts. (*a*) Sulfate self-exchange flux. *Ordinate:* Sulfate self-exchange flux $\vec{J}_{SO_4}$ (moles × min$^{-1}$ × *g* cells$^{-1}$). *Abscissa:* Extracellular sulfate concentration [$SO_4$] (mM). pH 7.2, 37 °C. (*b*) Chloride self-exchange flux. *Ordinate:* Chloride self-exchange flux $\vec{J}_{Cl}$ (moles × min$^{-1}$ × *g* cells$^{-1}$). *Abscissa:* Extracellular chloride concentration [Cl] (mM); pH 7.2; 0 °C. The concentration of ghosts corresponds to the cell concentration of a 10% (w/v) cell suspension. The concentration of either sulfate or chloride was varied by substituting isoosmotic amounts of $K_2SO_4$ for KCl

blood cells and red blood cell ghosts were incubated in phosphate buffer sucrose solutions containing various amounts of sulfate. Under these conditions, changes in cell volume have to be tolerated. According to the studies of Deuticke (1967, 1970) and Dalmark (1975), volume changes *per se* do not affect the anion permeability of the red blood cells. In order to prevent hemolysis at low tonicities, the dialysis technique of Cass and Dalmark (1973) was used. Instead of nystatin, amphotericin B was employed which at low concentrations renders the cells leaky for sodium and potassium without appreciably affecting the sulfate and the chloride permeabilities (Table 1) (for details *cf.*: Deuticke, Kim & Zöllner, 1973).

Fig. 3*a* exhibits the effect of sulfate concentration upon the sulfate self-exchange flux of intact red cells which were treated with amphotericin B. The sulfate flux is again plotted as a function of the extracellular sulfate concentration. The concentration responsiveness of the sulfate self-exchange flux differs substantially from the concentration dependence observed in the substitution experiments. The sulfate flux initially increases as the sulfate concentration is raised, reaching a maximum at

Table 1. Effect of amphotericin B on the sulfate self-exchange flux, chloride self-exchange flux and potassium efflux of human red blood cells[a]

| Amphotericin B µg/ml | $\vec{J}_{SO_4}$ moles × $min^{-1} \times g\ cells^{-1}$ | $\vec{J}_{Cl}$ moles × $min^{-1} \times g\ cells^{-1}$ | K-Efflux moles × $min^{-1} \times g\ cells^{-1}$ |
|---|---|---|---|
| 0 | $4.15 \cdot 10^{-6}$ | $2.68 \cdot 10^{-5}$ | $1.5 \cdot 10^{-8}$ |
| 0 | $4.29 \cdot 10^{-6}$ | $2.61 \cdot 10^{-5}$ | – |
| 2.5 | $4.52 \cdot 10^{-6}$ | $2.72 \cdot 10^{-5}$ | $3.2 \cdot 10^{-7}$ |
| 5.0 | $4.85 \cdot 10^{-6}$ | $2.65 \cdot 10^{-5}$ | $7.7 \cdot 10^{-7}$ |
| 10.0 | $5.22 \cdot 10^{-6}$ | $2.54 \cdot 10^{-5}$ | $1.56 \cdot 10^{-6}$ |

[a] The sulfate self-exchange flux $\vec{J}_{SO_4}$ was measured at 37 °C, pH 7.2. Cell concentration: 10% (w/v). Incubation solution (in mM) 94 $K_2SO_4$, 25 K-phosphate buffer, 30 sucrose. The chloride self-exchange flux $\vec{J}_{Cl}$ was measured at 0 °C, pH 7.2. Cell concentration: 1% (w/v). Incubation solution (in mM) 117 KCl, 25 K-phosphate buffer, 30 sucrose. The potassium efflux was determined at 37 °C, pH 7.2 by incubating the cells in a 165 mM NaCl solution. The fluxes were calculated from the initial potassium loss. Cell concentration: 10% (w/v).

sulfate concentrations between 100 and 300 mM. The concentration dependence of the flux depends strongly upon pH. At pH 6.3, the fluxes are much higher than at pH 8.5 and the concentration maximum of the flux is more pronounced. With increasing pH, the fluxes decrease and the peak of the flux curves shifts towards higher sulfate concentrations. Similar experiments were run with erythrocytes which had not been treated with amphotericin B. In these experiments, the sulfate concentration was varied from 50 mM up to 200 mM. A saturation of the sulfate self-exchange flux was likewise observed.

In intact red blood cells, the distribution ratio of anions and of hydrogen ions is strongly affected by the charge of the hemoglobin. Due to the Donnan effect, the intracellular anion concentrations and the intracellular pH can differ appreciably from the anion concentration and the pH of the extracellular solution. These differences are negligible if the experiments are performed with red blood cell ghosts. As shown in Fig. 3*b*, erythrocyte ghosts exhibit the same pattern of concentration responsiveness of the sulfate self-exchange flux as intact red blood cells. This indicates that the saturation of the self-exchange flux reflects a property of the erythrocyte membrane and cannot be attributed to secondary effects.

For the analysis of the sulfate flux/concentration curves, plotting procedures were employed which are common in enzyme kinetics (Webb, 1963). As an example, Fig. 4 displays the graphical examination of the

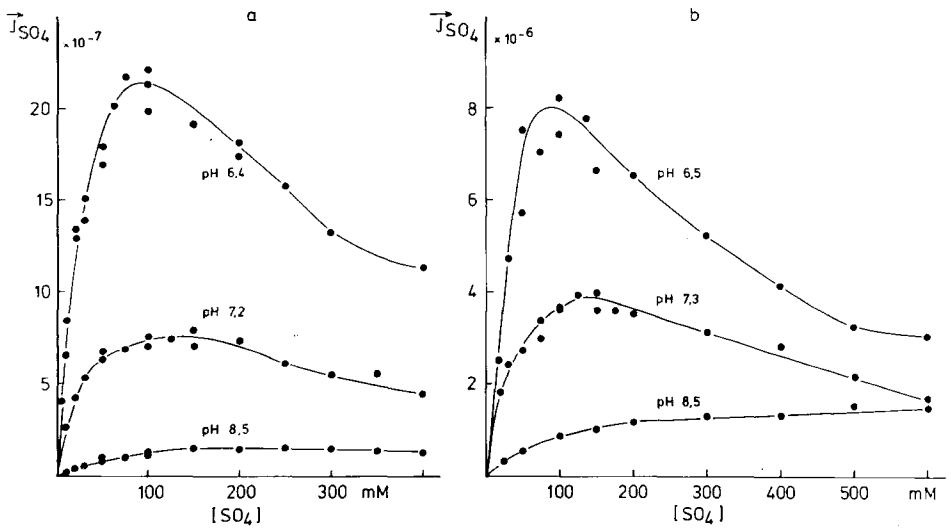


Fig. 3. Concentration dependence of the sulfate self-exchange flux of amphotericin B treated red blood cells (*a*) and red blood cell ghosts (*b*). (*a*) Amphotericin B treated red blood cells (25 °C). *Ordinate:* Sulfate self-exchange flux $\vec{J}_{SO_4}$ (moles × $min^{-1}$ × *g* $cells^{-1}$). *Abscissa:* Extracellular sulfate concentration [$SO_4$] (mM). pH as denoted at the respective curves. Cell concentration 10% (w/v). Incubation solution: 23 mM K-phosphate buffer, 30 mM sucrose, *x* mM $K_2SO_4$ as indicated on the abscissa, and 5 μg/ml amphotericin B. (*b*) Erythrocyte ghosts (37 °C). *Ordinate:* Sulfate self-exchange flux $\vec{J}_{SO_4}$ (moles × $min^{-1}$ × *g* $cells^{-1}$). *Abscissa:* Extracellular sulfate concentration [$SO_4$] (mM). pH as indicated in the figure. The concentration of ghosts corresponds to the cell concentration of a 10% (w/v) cell suspension. Incubation solution: 23 mM K-phosphate buffer, 30 mM sucrose, and *x* mM $K_2SO_4$ as indicated on the abscissa

flux/concentration curves of amphotericin B treated red blood cells. From the ascending branches of the flux curves a Lineweaver-Burk plot was made by plotting the reciprocal sulfate flux *vs.* the reciprocal of the extracellular sulfate concentration. The apparent half-saturation constant $K_s$ and the maximal sulfate flux $\vec{J}_{max(SO_4)}$ were supplied by the intercepts on the $1/[SO_4]$ and the $1/\vec{J}_{SO_4}$ axes, respectively. Dixon plots were made from the descending branches of the flux/concentration curves. The apparent self-inhibition constant $K_{is}$ is obtained from the intersection of the straight lines with the abscissa (Fig. 4*b*). The determination of the self-inhibition constant runs into difficulties if only a few points are available on the descending branch of the flux/concentration curve. In order to increase the accuracy of the plotting procedure, the intercepts on the $1/\vec{J}_{SO_4}$ axis obtained from the respective Lineweaver-Burk plots were inserted as additional points.

The graphically determined constants are compiled in Table 2. $K_s$, $K_{is}$ and $\vec{J}_{max(SO_4)}$ are functions of pH. $\vec{J}_{max(SO_4)}$ increases gradually as the

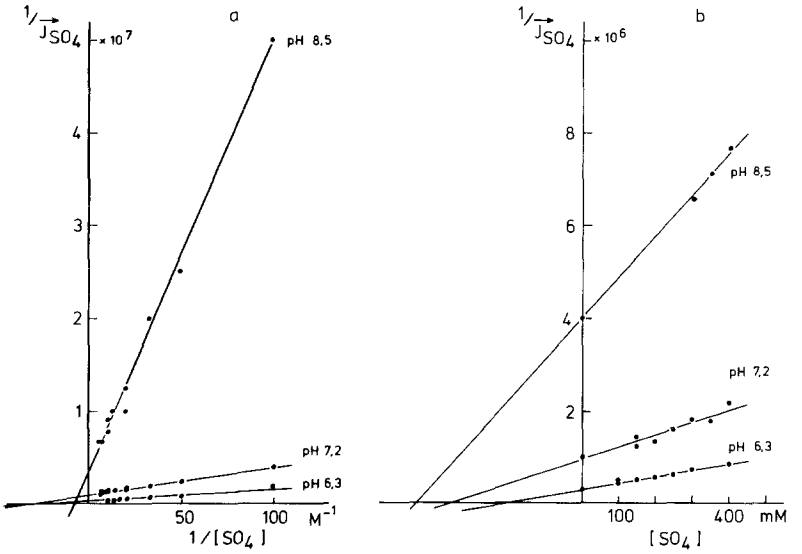


Fig. 4. Graphical evaluation of the flux/concentration curves. (*a*) Lineweaver-Burk plot made from the ascending branches of the flux/concentrations curves shown in Fig. 3*a*. *Ordinate:* Reciprocal sulfate self-exchange flux $1/\vec{J}_{SO_4}$ (*g* cells × min × moles$^{-1}$). *Abscissa:* Reciprocal of the extracellular sulfate concentration $1/[SO_4]$ (M$^{-1}$). (*b*) Dixon plot made from the descending branches of the flux/concentration curves shown in Fig. 3*a*. *Ordinate:* Reciprocal sulfate self-exchange flux $1/\vec{J}_{SO_4}$ (*g* cells × min × moles$^{-1}$). *Abscissa:* Extracellular sulfate concentration $[SO_4]$ (mM)

pH is lowered from 8.5 to 6.3. The actually observed maximal sulfate self-exchange flux is always 30–40% smaller than $\vec{J}_{max(SO_4)}$ (*cf:* Fig. 3*a* and *b*). The apparent half-saturation constant $K_s$ and the apparent self-inhibition constant $K_{is}$ decrease with decreasing pH. $K_s$ is strongly modified as the pH is reduced from 8.5 to 7.2 and little affected if pH is further reduced to 6.3. Conversely, $K_{is}$ decreases progressively over the whole pH range studied. At pH 7.2, the apparent half-saturation constant amounts to about 30 mM. The apparent self-inhibition constant is approximately one order of magnitude greater than the apparent half-saturation constant.

### *The pH-Dependence of the Sulfate Self-Exchange Flux*

Both the sulfate and the chloride self-exchange fluxes are strongly pH-dependent and exhibit pH-maxima at pH 6.2 and 7.8, respectively (Schnell, 1972; Gunn *et al.*, 1973; Wieth *et al.*, 1973; Wood & Passow, 1972; Dalmark, 1975). The pH-responses of the chloride self-exchange flux in intact red blood cells and in red blood cell ghosts display con-

Table 2. Graphical evaluation of the sulfate exchange flux curves[a]

| pH | $K_s$ (M) | $K_{is}$ (M) | $\vec{J}_{max(SO_4)}$ (moles $\times$ min$^{-1}$ $\times$ g cells$^{-1}$) |
|---|---|---|---|
| Amphotericin B (5 μg/ml) pretreated red blood cells (25°) | | | |
| 6.4 | $3.0 \cdot 10^{-2}$ | $2.1 \cdot 10^{-1}$ | $3.33 \cdot 10^{-6}$ |
| 7.2 | $3.0 \cdot 10^{-2}$ | $3.5 \cdot 10^{-1}$ | $9.9 \cdot 10^{-7}$ |
| 8.5 | $1.25 \cdot 10^{-1}$ | $4.5 \cdot 10^{-1}$ | $2.5 \cdot 10^{-7}$ |
| Red blood cell ghosts (37 °C) | | | |
| 6.5 | $3.6 \cdot 10^{-2}$ | $2.2 \cdot 10^{-1}$ | $1.12 \cdot 10^{-5}$ |
| 7.3 | $4.0 \cdot 10^{-2}$ | $5.0 \cdot 10^{-1}$ | $4.76 \cdot 10^{-6}$ |
| 8.5 | $1.14 \cdot 10^{-1}$ | – | $1.76 \cdot 10^{-6}$ |

[a] The experiments shown in Fig. 3 were used. The half-saturation constant $K_s$ of the sulfate self-exchange flux and the maximal sulfate flux $\vec{J}_{max(SO_4)}$ were determined by using a Lineweaver-Burk plot as shown in Fig. 4*a*, the self-inhibition constant $K_{is}$ was obtained from Dixon plots as shown in Fig. 4*b*

spicuous differences. The chloride self-exchange flux in intact cells increases as pH is raised from about 5–7, however, in contrast to intact cells, the ghosts do not show a decrease of the flux above pH 8 (Funder & Wieth, 1975). In contrast to the chloride self-exchange, the sulfate self-exchange in intact red cells and red cell ghosts exhibits the same pattern of pH-responsiveness (Figs. 5 and 6).

Fig. 5 displays the pH-dependence of the sulfate self-exchange flux of intact red blood cells. The sulfate flux is plotted *vs.* the extracellular pH. In these experiments the sulfate concentration was varied by substituting sulfate for chloride. The pH-profiles of the sulfate self-exchange flux are little affected by variations of the sulfate concentration. The pH maximum of the curves is positioned at about pH 6.2 and shows a slight shifting towards higher pH as the sulfate concentration is raised (Fig. 5*a*). The logarithmic plots ($\log \vec{J}_{SO_4}$ *vs.* pH) reveal a nearly parallel shift of the curves. The alkaline branches of the flux curves can be fitted by straight lines which have approximately the same slope ($\Delta \log \vec{J}_{SO_4}/\Delta \mathrm{pH} = -0.86$). The slopes of the acidic branches of the curves seem to be different, but they cannot be reliably determined (Fig. 5*b*).

Fig. 6*a* exhibits the pH-profile of the sulfate self-exchange flux in red cell ghosts. The sulfate concentration again was raised by adding sulfate in exchange for chloride. Erythrocyte ghosts exhibit the same pattern of pH-response as intact red cells, indicating that the pH-maximum of the sulfate self-exchange flux reflects a property of the cellular membrane. The logarithmic plots show that the flux/pH curves can be fitted by two straight lines (Fig. 6*b*). The alkaline branches of the flux

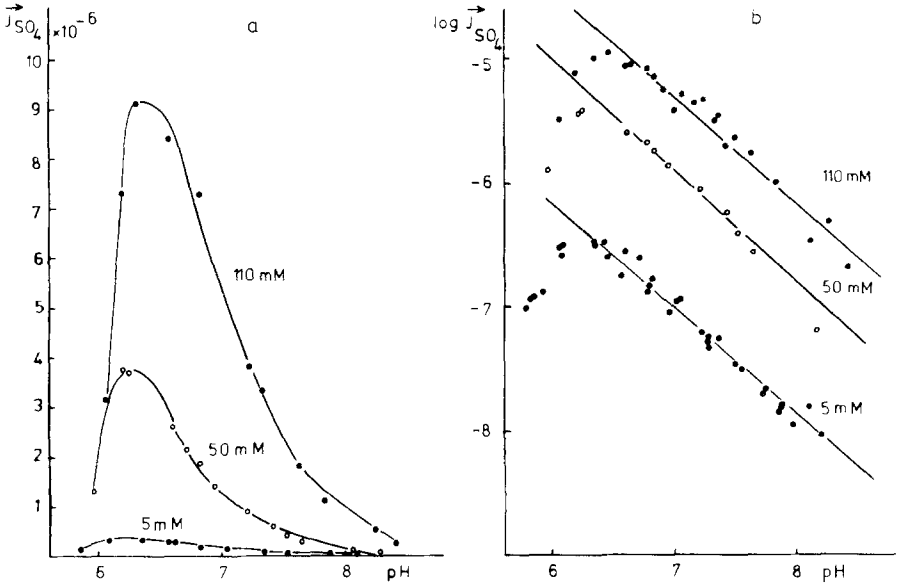


Fig. 5. pH-dependence of the sulfate self-exchange flux of intact red blood cells. *Ordinate* (*a*) Sulfate self-exchange flux $\vec{J}_{SO_4}$ (moles × $min^{-1}$ × *g* cells $^{-1}$), (*b*) log $\vec{J}_{SO_4}$ *Abscissa:* Extracellular pH. Incubation solutions (in mM): 5 $Na_2SO_4$, 150 NaCl; 50 $Na_2SO_4$, 75 NaCl; 110 $Na_2SO_4$, 16 NaCl. The sulfate concentrations are indicated in the figure. Cell concentration: 10% (w/v), 37 °C

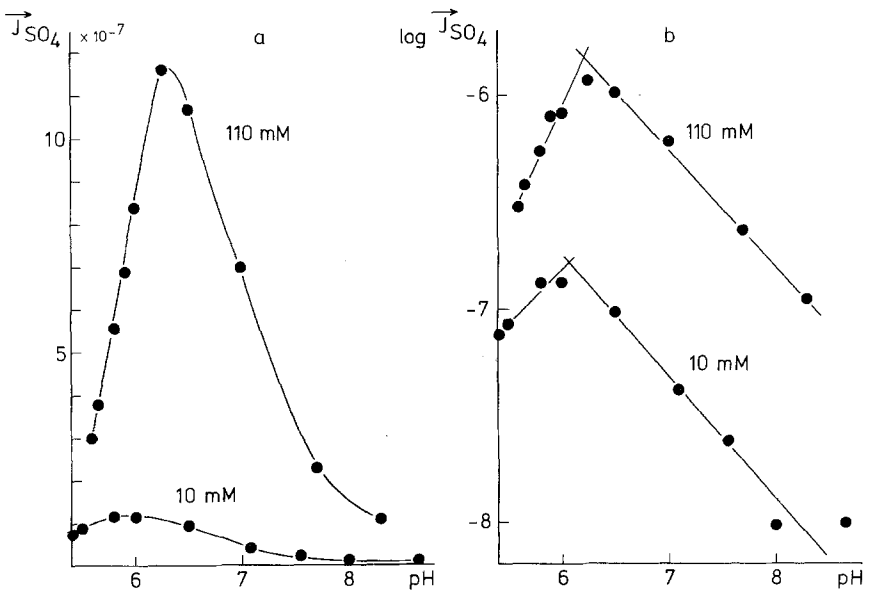


Fig. 6. pH-dependence of the sulfate self-exchange flux of red blood cell ghosts. *Ordinate:* (*a*) Sulfate self-exchange flux $\vec{J}_{SO_4}$ (moles × $min^{-1}$ × *g* $cells^{-1}$), (*b*) log $\vec{J}_{SO_4}$ *Abscissa:* Extracellular pH. Incubation solutions (in mM): 10 $K_2SO_4$, 23 K-phosphate buffer, 115 KCl, 30 sucrose (lower curve); 110 $K_2SO_4$, 23 K-phosphate buffer, 30 sucrose (upper curve). The sulfate concentrations are noted at the respective curves. Cell concentration: 10% (w/v), 25 °C

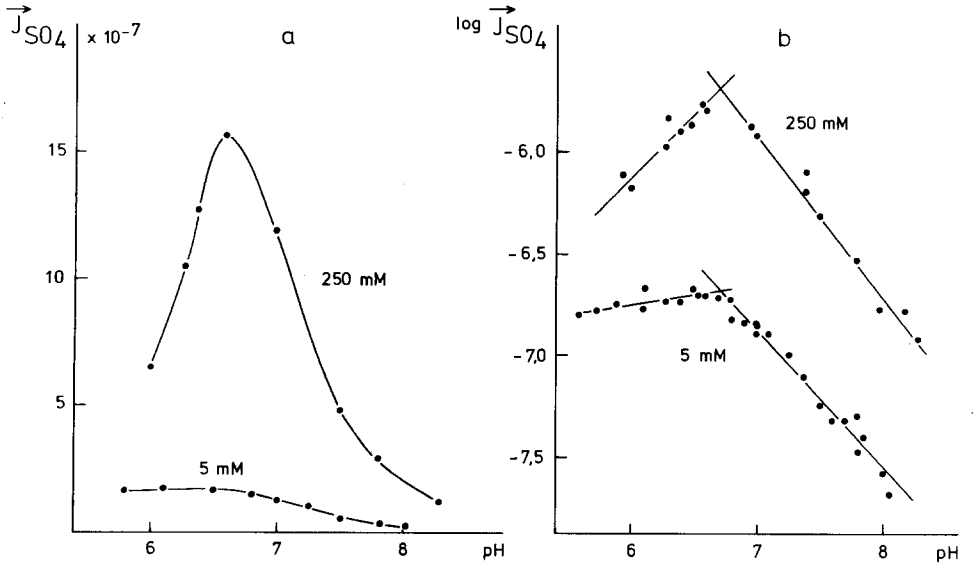


Fig. 7. pH-dependence of the sulfate self-exchange flux of chloride-free red blood cells treated with amphotericin B. *Ordinate:* (*a*) sulfate self-exchange flux $\vec{J}_{SO_4}$ (moles × min$^{-1}$ × *g* cells$^{-1}$). *Abscissa:* Extracellular pH. Incubation solutions: 5 mM $K_2SO_4$, 23 mM K-phosphate buffer, 30 mM sucrose, 5 µg/ml amphotericin B (lower curve); 250 mM $K_2SO_4$, 23 mM K-phosphate buffer, 30 mM sucrose, 5 µg/ml amphotericin B (upper curve). Cell concentration: 10% (w/v), 25 °C. The sulfate concentration is noted at the respective curves

curves again have approximately the same slope ($\Delta \log \vec{J}_{SO_4}/\Delta pH = -0.55$). The slopes of the acidic branches of the flux curves are distinctly different and amount to 0.53 and 1.14 at a sulfate concentration of 10 and 110 mM, respectively. Slight differences in the sulfate self-exchange flux in intact red blood cells and red blood cell ghosts can be observed above pH 6.5. In that pH-range, the sulfate fluxes in red cell ghosts are slightly higher than the sulfate fluxes in intact red cells under comparable conditions. These slight differences can possibly be attributed to pH-dependent changes of the Donnan distribution of the sulfate anions.

According to the studies of Dalmark (1975), the pH-dependence of the chloride self-exchange flux changes with the chloride concentration of the incubation solution. The pH-maximum of the chloride self-exchange flux is most pronounced at a low chloride concentration and disappears gradually as the chloride concentration is raised. In contrast, the pH-dependence of the sulfate self-exchange flux is little affected by variations of the sulfate concentration. Fig. 7 shows the sulfate self-exchange flux of amphotericin B-treated cells, which have been depleted of chloride. The pH-peak at high sulfate concentrations is more pronounced than at

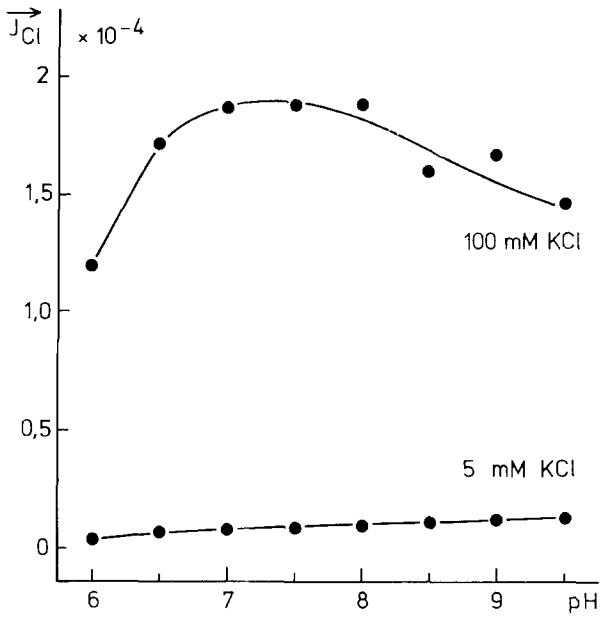


Fig. 8. The effect of sulfate on the pH-dependence of the chloride self-exchange flux of red blood cells. *Ordinate:* Chloride self-exchange flux $\vec{J}_{Cl}$ (moles × $min^{-1}$ × $g$ $cells^{-1}$). *Abscissa:* Extracellular pH. The experiments were performed with amphotericin B treated red blood cells. Incubation solutions: 100 mM KCl, 23 mM K-phosphate buffer, 60 mM sucrose, 5 µg/ml amphotericin B (upper curve); 5 mM KCl, 78 mM $K_2SO_4$, 23 mM K-phosphate buffer, 60 mM sucrose, 5 µg/ml amphotericin B (lower curve). 0 °C. Cell concentration: 1% (w/v). The chloride concentration is noted at the respective curves

low sulfate concentrations (Fig. 7*a*). The slopes ($\Delta \log \vec{J}_{SO_4}/\Delta$ pH) of the alkaline branch of the flux/pH curves amount to −0.66 (5 mM $K_2SO_4$) and to −0.78 (250 mM $K_2SO_4$) and are slightly different. It remains unclear as to whether these differences are significant or not. The slopes of the acidic branches of the flux/pH curves are significantly different and amount to 0.58 (250 mM $K_2SO_4$) and 0.08 (5 mM $K_2SO_4$), respectively (Fig. 7*b*).

The pH-dependence of the sulfate self-exchange is little affected by the addition of chloride (Figs. 5 and 6). Conversely, the pH-profile of the chloride exchange flux is strongly altered by the addition of sulfate (Fig. 8). In the absence of sulfate, the chloride self-exchange of amphotericin B treated cells displays a maximal flux at pH 7.5. By replacing most of the chloride with sulfate, the pH-maximum of the chloride exchange flux disappears and the chloride fluxes increase within the pH-range from 5–9.5. The apparent ionization constants $K_H$ and $K_{iH}$ and the maximal sulfate flux $\vec{J}_{max\,(SO_4/pH)}$ were graphically determined. The graphical

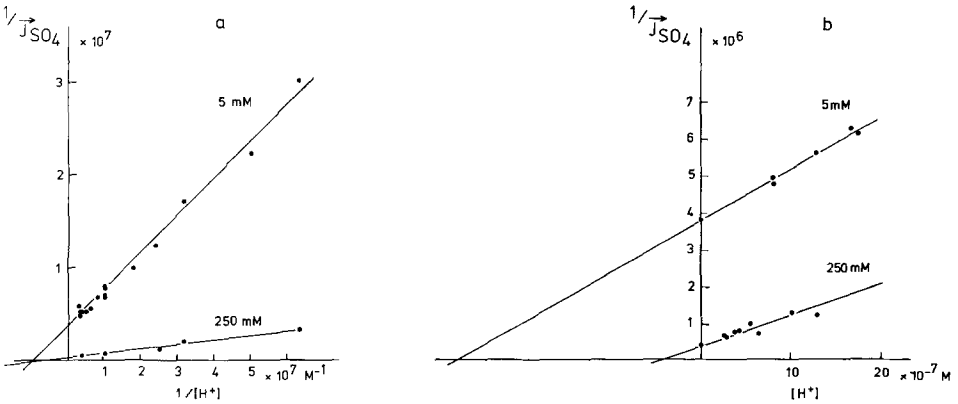


Fig. 9. Graphical evaluation of the flux/pH curves. (*a*) *Ordinate:* Reciprocal of the sulfate self-exchange flux $1/\vec{J}_{SO_4}$ (*g* cells × min × moles$^{-1}$). *Abscissa:* Reciprocal of the extracellular proton concentration $1/[H^+]$ ($M^{-1}$). (*b*) *Ordinate:* Reciprocal of the sulfate self-exchange flux $1/\vec{J}_{SO_4}$ (*g* cells × min × moles$^{-1}$). *Abscissa:* Extracellular proton concentration $[H^+]$ (M). The data were taken from Fig. 7. The sulfate concentrations are noted at the respective curves

examination of the flux/pH curves is shown in Fig. 9. The apparent ionization constant $K_H$ and the maximal sulfate flux $\vec{J}_{max\,(SO_4/pH)}$ were obtained by plotting the reciprocal sulfate flux *vs.* the reciprocal of the extracellular proton concentration.

At low proton concentrations, the double reciprocal plots yielded an almost linear relation between $1/\vec{J}_{SO_4}$ and $1/[H^+]$. $K_H$ and $\vec{J}_{max\,(SO_4/pH)}$ were supplied by the intercepts on the $1/[H^+]$ and $1/\vec{J}_{SO_4}$ axes, respectively. In most experiments, the inhibition of the sulfate self-exchange became apparent before the pH-maximum was reached and the curves bent upwards as they approached the ordinate. $K_{iH}$ was determined by plotting the reciprocal flux $1/\vec{J}_{SO_4}$ *vs.* the extracellular proton concentration $[H^+]$ (Fig. 9*b*). $K_{iH}$ was obtained from the intersections of the straight lines and the abscissa. For technical reasons, the determination of $K_{iH}$ is difficult. In most of the cases investigated, only a few points below pH 6.2 are available since at low pH, hemolysis occurs if no special precautions are taken. Again, the intercepts on the $1/\vec{J}_{SO_4}$ axis obtained from the double reciprocal plots were inserted as additional points.

In addition, an estimate of $K_{iH}$ can be made from the position of the pH-optimum of the flux curves, provided that $K_H$ is known. If the transport system is nearly saturated, the following relation holds true (Webb, 1963, p. 661):

$$pH_{opt} = 1/2\ (pK_H + pK_{iH})$$

Table 3. Constants obtained by the graphical evaluation of the flux/pH curves shown in Figs. 6*a*, 7*a* and 8*a*[a]

| $SO_4$ (mM) | $K_H$ (M) | $K_{iH}$ (M) | $\vec{J}_{max(SO_4/pH)}$ (moles × min$^{-1}$ × g cells$^{-1}$) |
|---|---|---|---|
| I. Erythrocytes (37 °C) | | | |
| 5 | $6.7 \cdot 10^{-7}$ | $(9.6 \cdot 10^{-7})$ | $8.3 \cdot 10^{-7}$ |
| 50 | $3.3 \cdot 10^{-7}$ | $(1.2 \cdot 10^{-6})$ | $6.2 \cdot 10^{-6}$ |
| 110 | $1.7 \cdot 10^{-7}$ | $(1.5 \cdot 10^{-6})$ | $1.43 \cdot 10^{-5}$ |
| II. Erythrocyte ghosts (25 °C) | | | |
| 10 | $1.3 \cdot 10^{-7}$ | $8.0 \cdot 10^{-6}$ | $1.44 \cdot 10^{-7}$ |
| 110 | $1.0 \cdot 10^{-7}$ | $3.2 \cdot 10^{-6}$ | $1.34 \cdot 10^{-6}$ |
| III. Amphotericin B treated red blood cells (25 °C) | | | |
| 5 | $1.5 \cdot 10^{-7}$ | $2.7 \cdot 10^{-6}$ | $2.63 \cdot 10^{-7}$ |
| 250 | $1.1 \cdot 10^{-7}$ | $4.5 \cdot 10^{-7}$ | $2.52 \cdot 10^{-6}$ |

[a] The apparent ionization constant $K_H$ and the maximal sulfate flux $\vec{J}_{max(SO_4/pH)}$ were obtained from the alkaline branches of the flux curves as shown in Fig. 9*a*. The ionization constant $K_{iH}$ was obtained from the acidic branches of the flux curves as shown in Fig. 9*b*. The values in brackets were computed from the location of the pH-optimum of the sulfate self-exchange flux.

$pH_{opt}$ is the pH at which the flux optimum is located. $pK_H$ and $pK_{iH}$ are the pK's referring either to the transport sites or to the inhibitor sites. $K_H$ can be accurately determined by means of the plotting procedures. The precise location of the flux maximum, however, is difficult to determine and small shifts of the pH-maximum can easily escape detection. Hence, the calculation of $K_{iH}$ by using the above equation is subject to a considerable error.

The constants obtained from the graphical analysis of the experiments shown in Figs. 5–7 are tabulated in Table 3. $K_H$, which can be reliably determined by the plotting procedures, ranges from $1 \times 10^{-7}$ M up to $7 \times 10^{-7}$ M. $K_H$ decreases slightly with increasing sulfate concentration irrespective of whether the sulfate concentration is raised by substituting sulfate for chloride or is raised without maintaining isotonicity. As far as it can be determined with sufficient accuracy, $K_{iH}$ also seems to decrease with increasing sulfate concentration. $\vec{J}_{max(SO_4/pH)}$ is the maximal theoretical sulfate flux at infinite hydrogen-ion concentration, if no inhibition of the sulfate selfexchange by protons would occur. Again, $\vec{J}_{max(SO_4/pH)}$ is 30–40% higher than the actually measured highest sulfate fluxes (compare Table 3 to Figs. 5–7).

### *The Effect of Some Monovalent and Divalent Anions on the Chloride and The Sulfate Self-Exchange Fluxes*

Some experimental findings suggest that in spite of the large differences in the exchange rates, sulfate and chloride are transported by the same anion transport system. The studies of Deuticke (1970) and of Wieth (1970), in particular, have shown that the phosphate and the sulfate self-exchanges are modified by other anions present in the incubation solution. The precise mode of action of these anions on the phosphate or the sulfate self-exchange has not yet been resolved.

Fig. 10 displays the inhibition of the sulfate self-exchange flux by chloride and the inhibition of the chloride self-exchange flux by sulfate. For technical reasons, the experiments were conducted with amphotericin B treated red blood cells. The fluxes were measured at Donnan equilibrium using radioactive isotopes as tracers (for details *cf:* Materials and Methods), and plotted *vs.* the extracellular concentrations of the inhibiting anions (Fig. 10*a* and *c*). Nearly hyperbolic dose-response curves were obtained. From these dose-response curves, Dixon plots were made (Fig. 10*b* and *d*). At low concentrations of the inhibiting anion, a linear relation between the reciprocal flux of the transported anion and the concentrations of the inhibiting anions was observed. At high concentrations of the inhibiting anions, systematic deviations do appear and the curves bend slightly upwards. The straight lines, fitting the data at low concentrations of the inhibiting anions, intersect above the abscissa, indicating a competitive type of inhibition. The apparent inhibitor constants $K_i$ were obtained from the intersections of the straight lines.

The graphically determined inhibitor constants are tabulated in Tables 4 and 5. The inhibitor constants for the sulfate self-exchange increase in the sequence $NO_3^- < Cl < (acetate)^- \simeq (oxalate)^{2-} < HPO_4^{2-}$. Correspondingly, the inhibitor constants of the chloride self-exchange were found to increase in the order of $SCN^- \simeq NO_3^- < SO_4^{2-} < HPO_4^{2-}$. From the anions tested, nitrate and thiocyanate exhibited the strongest inhibitory effect upon the sulfate and the chloride self-exchange. The inhibitory effect of the phosphate in both cases is surprisingly weak. In all cases, a competitive type of inhibition was observed.

The sulfate and the chloride self-exchange fluxes have different pH-profiles. If sulfate and chloride are transported by the same transport system, the affinities of both anion species to the transport system should change with pH. It therefore seems interesting to study the inhibitory

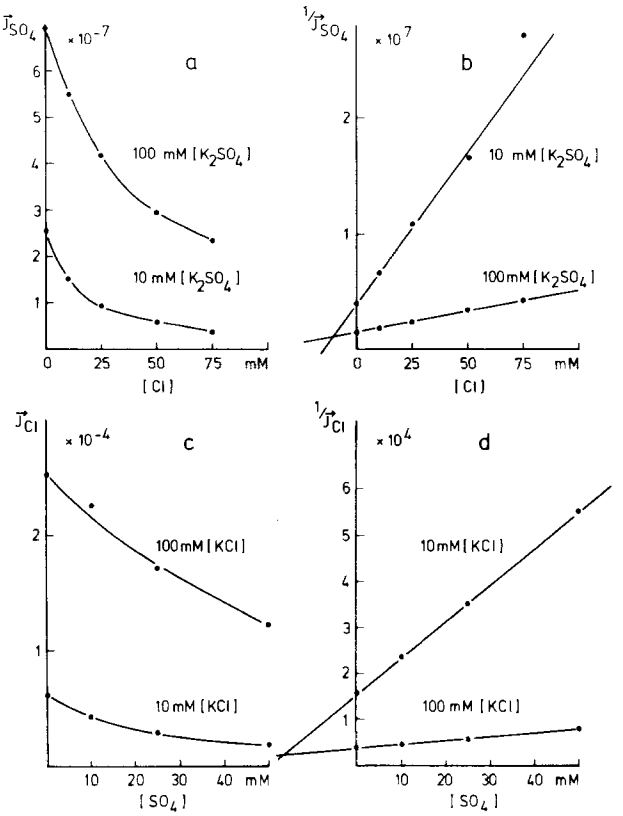


Fig. 10. Competition between sulfate and chloride. (*a,b*). Inhibition of the sulfate self-exchange flux by chloride. (*a*) Dose response curves. *Ordinate:* Sulfate self-exchange flux $\vec{J}_{SO_4}$ (moles × $min^{-1}$ × *g* cells $^{-1}$). *Abscissa:* Extracellular chloride concentrations [Cl] (mM). (*b*) Dixon plot made from the dose response curves shown in (*a*). *Ordinate:* Reciprocal of the sulfate self-exchange flux $1/\vec{J}_{SO_4}$ (*g* cells × min × $moles^{-1}$). *Abscissa:* Extracellular chloride concentration [Cl] (mM). 25 °C; pH 7.3. Cell concentration: 10% (w/v). (*c,d*) Inhibition of the chloride self-exchange flux by sulfate. (*c*) Dose response curves. *Ordinate:* Chloride self-exchange flux $\vec{J}_{Cl}$ (moles × $min^{-1}$ × *g* $cells^{-1}$). *Abscissa:* Extracellular sulfate concentration [$SO_4$] (mM). (*d*) Dixon plot made from the dose response curves shown in (*c*). *Ordinate:* Reciprocal of the chloride self-exchange flux $1/\vec{J}_{Cl}$ (*g* cells × min × $moles^{-1}$). *Abscissa:* Extracellular sulfate concentration [$SO_4$] (mM). Cell concentration during the $^{36}Cl$ back-exchange: 1% (w/v); pH 7.3; 0 °C. Incubation solutions: 5 µg/ml amphotericin B, 23 mM K-phosphate buffer, 60 mM sucrose, $K_2SO_4$ and KCl concentrations as indicated in the figure

effect of chloride on the sulfate transport and the inhibitory effect of sulfate on the chloride transport at differing pH. Again, hyperbolic dose response curves were obtained. The respective Dixon plots are shown in Fig. 11. The inhibition of the sulfate self-exchange flux by chloride

Table 4. Inhibition of the sulfate self-exchange by monovalent and divalent anions[a]

| Anion Species | n | $K_i$ (mM) |
|---|---|---|
| Nitrate | 3 | 3.8± 1.0 |
| Chloride | 4 | 13.9± 4.0 |
| Acetate | 4 | 25.9±11.3 |
| Oxalate | 4 | 22.6± 3.5 |
| Phosphate | 3 | 153.3±11.6 |

[a] The experiments were conducted in the same fashion as the experiments shown in Fig. 11. The inhibitor constant $K_i$ was determined graphically by means of a Dixon plot. Incubation solution: 10 and 100 mM $K_2SO_4$, respectively, 23 mM K-phosphate buffer, 30 mM sucrose, 5 μg/ml amphotericin B and increasing concentrations of the inhibiting anion species up to 100 mM. 25 °C, pH 7.2–7.3; cell concentration: 10% (w/v). n = number of experiments. $K_i$: mean value ± standard deviation.

Table 5. The inhibition of the chloride self-exchange[a]

| Anion species | n | $K_i$ (mM) |
|---|---|---|
| Thiocyanate | 3 | 1.5± 0.5 |
| Nitrate | 3 | 3.0±0.8 |
| Sulfate | 4 | 18.5± 4.4 |
| Phosphate | 3 | 130.7±15.4 |

[a] The chloride fluxes were measured as shown in Fig. 11. The inhibitor constants were determined by means of Dixon plots. Incubation solution: 10 or 100 mM KCl, respectively, 23 mM K-phosphate buffer, 30 mM sucrose, 5 μg/ml amphotericin B concentration of either $KNO_3$ or K-acetate, $K_2SO_4$ or K-phosphate up to 100 mM. pH 7.2–7.3, 0 °C. Cell concentration 1% (w/v). n = number of experiments. $K_i$: mean value ± standard deviation.

Table 6. pH-dependence of the inhibitor constants[a]

| | n | pH | $K_{i(SO_4)}$ (mM) |
|---|---|---|---|
| Chloride self-exchange (0 °C) | 3 | 6.1 | 15.7±0.7 |
| | 3 | 8.2 | 34.0±3.7 |
| | n | pH | $K_{i(Cl)}$ (mM) |
| Sulfate self-exchange (25 °C) | 4 | 6.0 | 45.3±2.1 |
| | 5 | 7.2 | 14.0±3.9 |

[a] The experiments were performed as indicated in Fig. 11. The inhibitor constants were graphically determined from the intersection of the straight lines. n = number of experiments. $K_i$: mean value ± standard deviation.

and of the chloride self-exchange flux by sulfate was always competitive. The graphically determined inhibitor constants are listed in Table 6.

The inhibitor constant of chloride $K_{i(Cl)}$ increases with increasing pH, indicating that at high pH the inhibitory effect of chloride on the sulfate transport is more pronounced than at low pH. Conversely, the

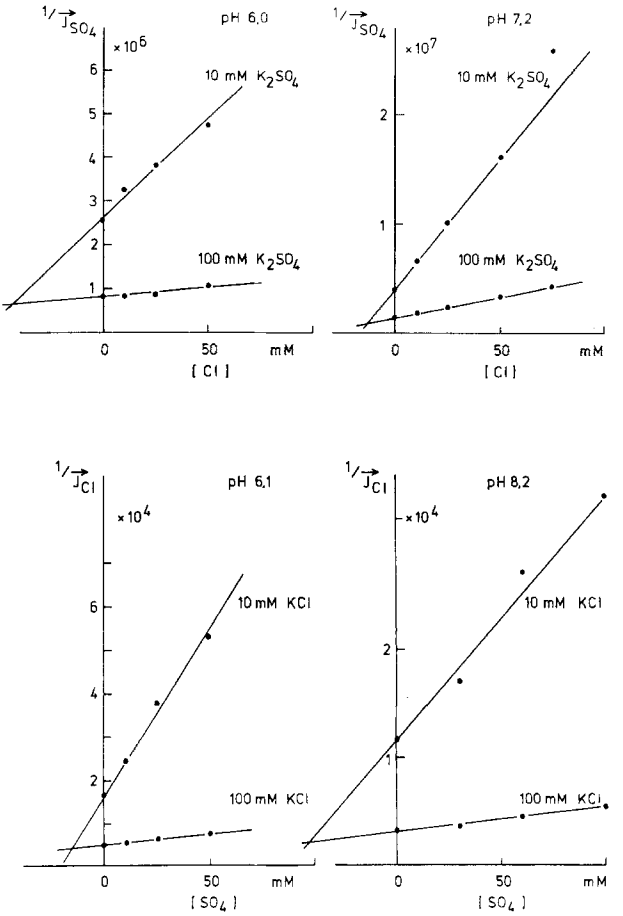


Fig. 11. Dixon plots showing the effect of pH on the competition between sulfate and chloride. *Ordinate:* Reciprocal of the sulfate self-exchange flux $1/\vec{J}_{SO_4}$ (*g* cells × min × moles$^{-1}$) or reciprocal chloride self-exchange flux $1/\vec{J}_{Cl}$ (*g* cells × min × moles$^{-1}$), respectively. *Abscissa:* Extracellular concentrations of chloride [Cl] (mM) or sulfate [$SO_4$] (mM), respectively. Incubation solutions: 5 µg/ml amphotericin B, 23 mM K-phosphate buffer, 60 mM sucrose, $K_2SO_4$ and KCl concentrations as indicated in the Figure. The sulfate self-exchange fluxes were measured at 25 °C, the cell concentration was 10% (w/v). The chloride flux measurements were conducted at 0 °C. The cell concentration during the $^{36}Cl$ back-exchange amounted to 1% (w/v). pH as denoted in the figure. The apparent inhibitor constants were obtained from the intersections of the straight lines

inhibitor constant of sulfate $K_{i\,(SO_4)}$ decreases with increasing pH, which means that the inhibitory effect of sulfate on the chloride transport decreases with increasing pH. The mutual competition between sulfate and chloride and the reverse pH-dependence of the relative affinities of both anions to the transport system strongly suggest that sulfate and chloride are transported by the same transport system.

## Discussion

### *Introductional Remarks*

The present paper deals with the kinetics of the sulfate transport across the red blood cell membrane. It results in the conclusion that the sulfate self-exchange flux is mediated by a "two-site transport mechanism". In order to characterize the sulfate transport, the concentration dependence, the pH-dependence and the effect of other anions on the sulfate self-exchange flux were studied. The experimental data were evaluated by using plotting procedures which are common in enzyme kinetics. Attempts were made to interpret the graphically determined constants within the frame of current concepts of the anion transport.

It is evident from a great number of experimental observations that the anion transport across the red blood cell membrane is mediated by a specific transport system, but the precise mechanism of the anion transport has remained unclear. The transport of anions across the red cell membrane is a complex reaction involving at least three separate steps. First the penetrating anion has to become adsorbed to one of the membrane surfaces. Subsequently, the anion is translocated across the membrane, and finally it is released at the opposite membrane surface.

The saturation of the sulfate self-exchange flux (Fig. 3) indicates that sulfate interacts with a limited number of "transport sites". At low sulfate concentrations, most of the transport sites are vacant and the sulfate self-exchange flux increases progressively as the sulfate concentration is raised. Depending upon pH, the sulfate self-exchange flux reaches a concentrations maximum at sulfate concentrations between 100 and 300 mM. At this concentration, the sulfate self-exchange is limited by the availability of transport sites.

At high sulfate concentrations the inhibition of the sulfate self-exchange flux prevails. In order to account for the self-inhibition, a second type of sites has to be introduced which are denoted "inhibitor sites". The inhibitor sites have a much lower affinity to sulfate than the transport sites. Therefore, at low sulfate concentrations, the inhibitor sites are empty. At high sulfate concentrations when most of the transport sites are saturated, the effect of the inhibitor sites on the sulfate transport predominates. The effect of pH on the flux concentration curves suggests that both types of sites are activated by protons.

In the substitution experiments, no saturation of the sulfate and of the chloride self-exchange fluxes was observed (Figs. 1 and 2). In these experiments, the increase of the sulfate or the chloride concentrations

was associated with a decrease of the concentration of a second anion species and the true concentration dependence of the sulfate and the chloride self-exchange flux is obscured.

In a similar fashion, the pH-maximum of the sulfate self-exchange flux can be explained by a two-site transport mechanism. If the pK of the transport sites is higher than the pK of the inhibitor sites, then at high pH the transport sites are first activated by protons and the sulfate flux increases as pH is reduced. At a further reduction of pH, an increasing fraction of inhibitor sites is activated. Below pH 6.2, the action of the inhibitor sites on the sulfate self-exchange predominates and the sulfate self-exchange flux is inhibited.

### *Problems of Graphical Analysis*

The graphical analysis of the flux measurements is based upon the following assumptions: (1) The translocation of anions across the membrane determines the rate of the sulfate and the chloride self-exchange. (2) The self-exchange fluxes are regulated from the outer membrane surface. (3) The effect of surface charge on the surface concentrations of ions can be disregarded.

*1. The rate-determining step.* There are several lines of evidence which indicate that the translocation of anions across the erythrocyte membrane is much slower than the reactions taking place at the membrane surfaces. (a) Assuming an effective membrane thickness of 50 Å and using the known diffusion coefficients of sulfate and chloride in water, the anion permeability of the erythrocyte membrane can be compared to the anion permeability of a water layer of corresponding thickness. The comparison shows that the sulfate permeability of the erythrocyte membrane at 25 °C is about 9 orders of magnitude smaller than the sulfate permeability of a 50 Å water layer, and that the chloride permeability of the erythrocyte membrane at 0 °C is about 7 orders of magnitude smaller than the chloride permeability of a 50 Å water layer. Even if one assumes that only 1/1000th of the total membrane area participates in the anion transport, the sulfate permeability of the transport system would be 6 orders of magnitude and the chloride permeability of the transport system would be 4 orders of magnitude smaller than the permeabilities of a water layer of corresponding thickness. This suggests that the translocation of anions across the membrane is the rate-determining process in anion exchange. (b) Sulfate and chloride are transported by the same transport

system. Both anions have about the same affinities to the transport system but the self-exchange fluxes of sulfate and chloride differ in about 5 orders of magnitude. The saturation of the sulfate and the chloride self-exchange fluxes indicate that at high concentrations the transport capacity of the anion transport system is limited by the availability of transport sites. If the adsorption of anions to the transport sites would be rate-determining for the transport of anions across the red blood cell membrane, the transport sites should be vacant and the self-exchange fluxes of sulfate and chloride should not saturate. The saturation of the anion self-exchange fluxes therefore indicates that not the adsorption but one of the consecutive reactions is rate-determining. If on the other hand the desorption of anions at the trans-membrane side should be rate-determining and responsible for the differences in the self-exchange fluxes, then the chloride flux should be completely blocked by the presence of sulfate. This however, is not observed. It is concluded therefore that the translocation and not the adsorption or the desorption of anions is rate-determining for the anion self-exchange flux.

2. *The regulation of the anion self-exchange flux.* We do not know whether the sulfate and the chloride self-exchange fluxes are regulated from the outer or from the inner membrane surface or whether both membrane surfaces are involved in the regulation of the anion transport. Since the self-exchange fluxes were measured at equilibrium conditions, the inward flux and the outward flux of sulfate or chloride are equal in magnitude. Experiments with nonpenetrating inhibitors seem to indicate that the sulfate and the chloride transports are primarily regulated from the outer membrane surface. We therefore decided to use the external concentrations of sulfate and chloride and the external pH for the graphical analysis of the data. In intact cells, the intracellular and the extracellular concentrations of sulfate and chloride and the intracellular and the extracellular pH can differ substantially depending upon the Donnan potential under the respective experimental conditions. For ghosts, the differences between intra- and extracellular anion concentrations and between intra- and extracellular pH should be negligible.

3. *The effect of surface charge on the anion transport.* The membrane surfaces carry a net electrical charge which gives rise to a surface potential. Therefore, the surface concentration of ions, in general, will differ from the concentrations of ions in the bulk solution. For the graphical analysis, the surface concentrations rather than the bulk concentrations

should be used, but the surface concentrations are not known. Experiments with amino group reagents have indicated that cationic groups such as amino groups, imido groups or guanido groups are involved in the regulation of the anion transport. These groups are supposed to be located in the immediate vicinity of the anion binding sites and are supposed to facilitate the binding of anions. We cannot decide from our experiments whether changes of the graphically determined constants reflect changes in the surface potentials or whether they indicate the activation of the membrane sites by protons.

### *Graphical Analysis of the Flux/Concentration Curves*

For the graphical examination of the sulfate flux/concentration curves, Lineweaver-Burk and Dixon plots were used (Fig. 4). The Lineweaver-Burk plots made from the ascending branches of the flux/concentration curves display a nearly linear relation between the reciprocal sulfate flux and the reciprocal sulfate concentration, indicating that, at a first approximation, the sulfate self-exchange flux at low sulfate concentrations adheres to a Michaelis Menten kinetics. The slope of the straight lines increases with increasing pH but the straight lines fitting the data do not intersect at one point. The apparent half-saturation constant $K_s$ should primarily reflect the interaction of sulfate with the transport sites. The apparent half-saturation constant at 25 °C was 30 mM (pH 6.4), 30 mM (pH 7.2), and 125 mM (pH 8.5), respectively (Table 2), pointing to the fact that at about pH 7 most of the transport sites seem to be activated by protons. The apparent self-inhibition constants $K_{is}$ at 25 °C were 210 mM (pH 6.3), 350 mM (pH 7.2), and 450 mM (pH 8.5), respectively, suggesting that an increasing fraction of the inhibitor sites is activated as pH is reduced from 8.5 to 6.4.

The decrease of $K_s$ and $K_{is}$ could indicate that protons are directly involved in the binding of sulfate to the transport and to the inhibitor sites. Alternatively, the decrease of $K_s$ and $K_{is}$ could reflect an increase of the surface concentrations of sulfate anions which is caused by an increase of the surface potential at the membrane surfaces as pH is reduced. For the time being, we cannot distinguish between both possibilities. $\vec{J}_{max(SO_4)}$ increases progressively as pH is reduced from 8.5 to 6.3. The concentration dependence of the sulfate self-exchange flux was studied at a pH which is located above the pH-maximum of the sulfate self-exchange flux. The occurence of a pH-maximum of $\vec{J}_{max(SO_4)}$ therefore, is not to be expected under our experimental conditions. It should be

noted, however, that a further increase of $\vec{J}_{max(SO_4)}$ was observed below pH 7. At that pH, all transport sites seem to be activated and the activation of the inhibitor sites increases. The increase of $\vec{J}_{max(SO_4)}$ points to the fact that the translocation is a function of pH. The maximal theoretical sulfate flux $\vec{J}_{max(SO_4)}$ is always considerably higher than the highest actually observed sulfate flux, indicating that an inhibitory process starts operating before the maximal theoretical transport capacity of the system is reached.

Accepting the published values of $2.5 \times 10^5$ sites per cell (Rothstein & Cabantchik, 1974), the turnover numbers for sulfate and chloride can be estimated. The turnover numbers for sulfate would be approximately 10 ions per site per sec at 25 °C and approximately 40 ions per site sec at 37 °C. These turnover numbers are much smaller than the turnover numbers of chloride which, according to the studies of Brahm (1975), amount to $1.9 \times 10^5$ ions per site per sec (38 °C).

### *Graphical Analysis of the Flux/pH Curve*

To further analyze the pH-dependence of the sulfate self-exchange flux, $\log \vec{J}_{SO_4}$ was plotted *vs.* pH. The slope ($\Delta \log \vec{J}_{SO_4} / \Delta$ pH) of the alkaline branches of the flux/pH curves is negative and ranges from $-0.55$ to $-0.86$. It is little affected by variations of the sulfate concentration. In erythrocyte ghosts, a slope of about $-0.5$ was observed, suggesting that 2 protons are required for the binding of 1 sulfate anion. In most cases, however, the slope was smaller than $-0.5$. This means that either less than 2 protons are required for the binding of 1 sulfate anion or that the translocation rate increases as pH is lowered.

The graphical determination of $K_H$, the ionization constant of the transport sites, requires (1) that all activated transport sites are saturated, (2) that the translocation is independent of pH, and (3) that the inhibitor sites are empty. It is immediately evident that the above conditions cannot be strictly met.

The plot $1/\vec{J}_{SO_4}$ *vs.* $1/[H^+]$ made from the alkaline branches of the sulfate flux/pH curves exhibits a nearly linear relation between the reciprocal sulfate flux and the reciprocal proton concentration. The straight lines fitting the data intersect on the abscissa (Fig. 9*a*). This indicates a noncompetitive activation, meaning that the binding of protons to the transport sites is not affected by the sulfate concentration. The apparent pK of the transport sites in erythrocyte ghosts and amphotericin B treated cells is around 7.0 at 25 °C. Since the translocation seems

to increase as pH is reduced, this would result in an overestimate of the apparent ionization constant. The graphically determined pK's therefore have to be considered as the lower limit of the true pK of the transport sites. At 37 °C, the pK seems to be positioned around 6.5 (Table 3).

The slope ($\Delta \log \vec{J}_{SO_4}/\Delta$ pH) of the acidic branches of the flux curve below pH 6.2 is considerably affected by variations of the sulfate concentration. The plots $1/\vec{J}_{SO_4}$ *vs.* $[H^+]$ show a mixed inhibition (Fig. 9*b*). The apparent ionization constant $K_{iH}$ of the inhibitor sites range from $4 \times 10^{-7}$ to $8 \times 10^{-6}$ M. $K_{iH}$ is considerably reduced as the sulfate concentration is raised (Table 3), suggesting that the binding of sulfate facilitates the binding of protons to the inhibitor sites. Again $\vec{J}_{max(SO_4/pH)}$ is considerably higher than the actually observed maximal sulfate flux, indicating that the inhibition starts before the maximal theoretical transport capacity of the system is reached.

### *Graphical Analysis of the Inhibition of the Sulfate and the Chloride Self-Exchange Flux*

To further examine the mechanism of the sulfate and the chloride transport, the action of some anions on the sulfate and the chloride self-exchange flux was studied. The Dixon plots revealed a linear relation between the reciprocal of the sulfate and the chloride flux, respectively, and the concentration of the inhibiting anion species. The point of intersection of the straight lines is placed distinctly above the abscissa indicating a competitive type of inhibition. Under our experimental conditions, the Dixon plots mainly reflect the competition of the transported anion and the inhibiting anion for the transport sites. As already mentioned, at high concentrations of the inhibiting anion species, deviations from linearity become apparent in the Dixon plots. It should be mentioned in this context, that amphiphilic inhibitors under comparable conditions show a noncompetitive type of inhibition of the sulfate and the chloride self-exchange fluxes (Schnell, 1972; Gerhardt *et al.*, 1973).

The inhibition constants, as graphically determined for the various anion species, display sizable differences. This points to the fact that the affinities of the anions to the transport sites are different. No simple correlation between the electrical charge of the anions and their inhibitory action on the sulfate or the chloride self-exchange flux was found, indicating that the interaction of the anions with the transport sites cannot simply be attributed to electrostatic forces. It appears that, in addition

to electrostatic forces, short range forces contribute to the binding of anions to the transport sites.

Furthermore it should be noted that no correlation between the rate of the self-exchange flux of the inhibiting anion species and its inhibitory action on the sulfate and the chloride self-exchange was observed. The self-exchange flux of chloride for instance is many orders of magnitude greater than the self-exchange flux of phosphate, but chloride has a greater inhibitory effect on the sulfate self-exchange than phosphate. These observations indicate that the interaction between the different anion species takes place at the membrane surfaces and not inside the membrane.

The mutual competition between sulfate and chloride strongly suggests that both anion species share a common transport system. Additional evidence for this conclusion is supplied by the observation that the relative affinities of chloride and sulfate to the transport system show a reverse pH-dependency. The inhibitory effect of chloride on the sulfate self-exchange increases with increasing pH. Conversely, the inhibitory effect of sulfate on the chloride self-exchange decreases as pH is elevated.

## *Final Remarks*

The concentration dependence and the pH-dependence of the sulfate self-exchange flux indicate that the sulfate transport across the erythrocyte membrane is mediated by a "two-site transport mechanism". The transport system could consist either of a mobile carrier (Gunn, 1972, 1973; Wieth, 1972, Gunn *et al.*, 1973) or of a two-site pore. The experiments reported in this paper do not permit making a distinction between both transport mechanisms. For theoretical details, the reader is referred to the papers of Lieb and Stein (1974*a*, 1974*b*).

Recent biochemical studies (Cabantchik & Rothstein, 1974*a*, 1974*b*; Rothstein, Cabantchik, Balshin & Juliano, 1975; Zaki, Fasold, Schuhmann & Passow, 1975) suggest that a membrane protein with a molecular weight of 95,000 daltons plays a decisive role in anion transport. The protein seems to span the membrane and to be in contact with the inner and the outer membrane surface. Such a protein could easily form a sort of anion permeable channel. If such a protein would act as a mobile carrier, the anion transport should be associated with conformation changes of the protein. Since the protein is embedded into a rather

rigid membrane structure, conformational changes are unlikely to occur under physiological conditions, yet they cannot be excluded.

The commonalities of the sulfate and the chloride self-exchange fluxes strongly suggest that both anion species are transported by the same transport system (*cf.* Results). This inference is corroborated by the competition between sulfate and chloride and by the observation that the self-exchange fluxes of both anion species are inhibited by the same agents. On the other hand, the sulfate and the chloride exhibit two important differences. First the chloride self-exchange at 37 °C (Brahm, 1975) is almost 5 orders of magnitude faster than the sulfate self-exchange. Secondly, the pH-optima for the sulfate and the chloride self-exchange fluxes are located at different pH. These differences, however, do not invalidate the above conclusion. The differences in the transport rates can be easily explained by assuming different translocation rates for sulfate and chloride. The different position of the pH-maxima can be accounted for by postulating that the binding of sulfate to the transport sites requires two protons, whereas for the binding of chloride only one proton is necessary (Gunn, 1973; Dalmark, 1975). Therefore, the pH-maximum of the sulfate self-exchange flux is expected to be located at a lower pH than the pH-maximum of the chloride self-exchange flux.

This work was supported by the Deutsche Forschungsgemeinschaft. We are indebted to Profs. C. Albers and W. Moll for their continuous interest in our investigations and for encouraging comments. In addition, we want to thank Dr. Reinhardt, Chemische Fabriken v. Heyden, for supplying amphotericin B.

## References

Bodemann, H., Passow, H. 1972. Factors controlling the resealing of the membrane of human erythrocyte ghosts after hypotonic hemolysis. *J. Membrane Biol.* **8**:1

Brahm, J. 1975. Chloride permeability in human red cells at 0–38 °C. V. *Int. Biophys. Congr. Copenhagen.* (Abstr.) 319

Cabantchik, Z.I., Rothstein, A. 1972. The nature of the membrane sites controlling anion permeability of human red blood cells as determined by studies with disulfonic stilbene derivatives. *J. Membrane Biol.* **10**:311

Cabantchik, Z.I., Rothstein, A. 1974*a*. Membrane proteins related to anion permeability of human red blood cells: I. Localization of disulfonic stilbene binding sites in proteins involved in permeation. *J. Membrane Biol.* **15**:207

Cabantchik, Z.I., Rothstein, A. 1974*b*. Membrane proteins related to anion permeability of human red blood cells: II. Effects of proteolytic enzymes on disulfonic stilbene sites of surface proteins. *J. Membrane Biol.* **15**:227

Cass, A., Dalmark, M. 1973. Equilibrium dialysis of ions in nystatin-treated red cells. *Nature New Biol.* **244**:47 (132)

Dalmark, M. 1972. The effect of temperature, bicarbonate-carbon dioxide, and pH on the chloride transport across the human red cell membrane. *In*: Oxygen Affinity of

Hemoglobin and Red Cell Acid-Base Status. M. Rørth and P. Astrup, editors. p. 320. Munksgaard, Copenhagen

Dalmark, M. 1975. Chloride transport in human red cells. *J. Physiol. (London)* **250**:39

Dalmark, M., Wieth, J.O. 1970. Chloride and sodium permeabilities of human red cells. *Biochim. Biophys. Acta* **219**:525

Dalmark, M., Wieth, J.O. 1972. Temperature dependence of chloride, bromide, iodide, thiocyanate and salicylate transport in human red cells. *J. Physiol. (London)*. **224**:583

Deuticke, B. 1967. Über die Kinetik der Phosphat-Permeation in den Menschen-Erythrozyten bei Variation von extracellulärer Phosphat-Konzentration, Anionen-Milieu und Zellvolumen. *Pflügers Arch.* **296**:21

Deuticke, B. 1970. Anion permeability of the red blood cell. *Naturwissenschaften* **57**:172

Deuticke, B., Kim, M., Zöllner, Chr. 1973. The influence of amphotericin B on the permeability of mammalian erythrocytes to nonelectrolytes, anions and cations. *Biochim. Biophys. Acta* **318**:345

Funder, J., Wieth, J.O. 1975. Comparison of chloride transport in human erythrocytes and ghosts. V. Int. Biophys. Congr. Copenhagen (Abstr.) 107

Gardos, G., Hoffman, J.F., Passow, H. 1969. Flux measurements in erythrocytes. *In*: Laboratory Techniques in Membrane Biophysics. H. Passow and R. Stämpfli, editors. p. 9. Springer-Verlag, Heidelberg

Gerhardt, S., Schnell, K.F. 1975. The inhibition of the anion netflux across the human erythrocyte membrane. *Pflügers Arch.* **355**:*R*74

Gerhardt, S., Schöppe-Fredenburg, A., Schnell, K.F. 1973. Inhibition of the sulfate transfer in human erythrocytes. *In*: Erythrocytes, Thrombocytes, Leukocytes. E. Gerlach, K. Moser, E. Deutsch, and W. Wilmans, editors. p. 87. Thieme-Verlag, Stuttgart

Gunn, R.B. 1972. A titrable carrier model for both mono- and divalent anion transport in human red cells. *In*: Oxygen affinity of hemoglobin and red cell acid base status. M. Rørth and P. Astrup, editors. p. 823. Munksgaard, Copenhagen

Gunn, R.B. 1973. A titrable carrier for monovalent and divalent inorganic anions in red blood cells. *In:* Erythrocytes, Thrombocytes, Leukocytes, E. Gerlach, K. Moser, E. Deutsch, and W. Wilmans, editor p. 77. Thieme-Verlag, Stuttgart

Gunn, R.B., Dalmark, M., Tosteson, D.C., Wieth, J.O. 1973. Characteristics of chloride transport in human red blood cells. *J. Gen. Physiol.* **61**:185

Gunn, R.B., Hartley, P.N., Horton, J.M. 1974. Sulfate transport in human red cells: Concentration dependence of sulfate flux. *Fed. Proc.* **33**:Abstr. 2086

Gunn, R.B., Tosteson, D.C. 1971. The effect of 2,4,6-trinitro-*m*-cresol on cation and anion transport in sheep red blood cells. *J. Gen. Physiol.* **57**:593

Hunter, M.J. 1971. A quantitative estimate of the nonexchange-restricted chloride permeability of the human red blood cell. *J. Physiol. (London)* **218**:49*P*

Knauf, P.A., Fuhrmann, G.F. 1974. Determination of chloride and sulfate conductance in human red blood cells. *Fed. Proc.* **33**:Abst. 2075

Knauf, P.A., Rothstein, A. 1971. Chemical modifications of membranes. I. Effects of sulfhydryl and amino reactive reagents on anion and cation permeability of the human red blood cell. *J. Gen. Physiol.* **58**:190

Lassen, U.V., Pape, L., Vestergaard-Bogind, B. 1973. Membrane potential of Amphiuma red cells: Effects of calcium. *In*: Erythrocytes, Thrombocytes, Leukocytes, E. Gerlach, K.Moser, E. Deutsch, and W. Wilmans, editors. p. 33. Thieme-Verlag, Stuttgart

Lepke, S., Passow, H. 1971. The permeability of the human red blood cell to sulfate ions. *J. Membrane Biol.* **6**:158

Lepke, S., Passow, H. 1972. The effect of pH at hemolysis on the reconstitution of low cation permeability in human erythrocyte ghosts. *Biochim. Biophys. Acta* **255**:696

Lieb, W.R., Stein, W.D. 1974*a*. Testing and characterizing the simple pore. *Biochim. Biophys. Acta* **373**:165

Lieb, W.R., Stein, W.D. 1974**b**. Testing and characterizing the simple carrier. *Biochim. Biophys. Acta* **373**:178

Obaid, A.L., Rega, A.F., Garrahan, P.J. 1972. The effects of maleic anhydride on the ionic permeability of red cells. *J. Membrane Biol.* **9**:385

Passow, H., Schnell, K.F. 1969. Chemical modifiers of passive ion permeability of the erythrocyte membrane. *Experientia* **25**:460

Poensgen, J., Passow, H. 1971. Action of 1-fluoro-2,4-dinitrobenzene on passive ion permeability of the human red blood cell. *J. Membrane Biol.* **6**:210

Rothstein, A., Cabantchik, Z.I. 1974. Protein structures involved in the anion permeability of the red blood cell membrane. *In*: Comparative Biochemistry and Physiology of Transport. L. Bolis, K. Bloch, S.E. Luria, F. Lynen, editors. p. 354. North-Holland Publishing Company, Amsterdam, London

Rothstein, A., Cabantchik, Z.I., Balshin, M., Juliano, R. 1975. Enhancement of anion permeability in lecithin vesicles by hydrophobic proteins extracted from red blood cell membranes. *Biochem. Biophys. Res. Commun.* **64**:144 (1)

Scarpa, A., Cecchetto, A., Azzone, G.F. 1970. The mechanism of anion translocation and pH equilibration in erythrocytes. *Biochim. Biophys. Acta* **219**:179

Schnell, K.F. 1972. On the mechanism of inhibition of the sulfate transfer across the human erythrocyte membrane. *Biochim. Biophys. Acta* **282**:265

Schnell, K.F., Gerhardt, S. 1973. The effect of the membrane potential on the anion exchange across the erythrocyte membrane. *Pflügers Arch.* **343**:*R*60

Schnell, K.F., Gerhardt, S. 1975. Kinetic studies of the anion transport across the red blood cell membrane. Vth Int. Biophys. Congr. (Copenhagen) *Abstr: P*-317

Tosteson, D.C., Gunn, R.B., Wieth, J.O. 1973. Chloride and hydroxyl ion conductance of sheep red cell membrane. *In*: Erythrocytes, Thrombocytes, Leukocytes. E. Gerlach, K. Moser, E. Deutsch, and W. Wilmans, editors. p. 62. Thieme-Verlag, Stuttgart

Webb, J.L. 1963. Enzyme and metabolic inhibitors. Vol. 1, p. 661 Academic press, New York

Wieth, J.O. 1970. Effect of some monovalent anions on chloride and sulfate permeability of human red blood cells. *J. Gen. Physiol.* **207**:581

Wieth, J.O. 1972. The selective ionic permeability of the red cell membrane. *In*: Oxygen affinity of hemoglobin and red cell acid base status. M. Rørth, and P. Astrup, editors. p. 265. Munksgaard, Copenhagen

Wieth, J.O., Dalmark, M., Gunn, R.B., Tosteson, D.C. 1973. The transfer of monovalent inorganic anions through the red cell membrane. *In*: Erythrocytes, Thrombocytes, Leukocytes. E. Gerlach, K. Moser, E. Deutsch, and W. Wilmans, editors. p. 71. Thieme-Verlag, Stuttgart

Wood, Ph.G., Passow, H. 1973. Some remarks on the current concepts of the mechanism of anion permeability. *In*: Proceedings of symposium on drugs and transport. B.A. Callingham, editor p. 149. MacMillan, London

Zaki, L., Fasold, H., Schuhmann, B., Passow, H. 1975. Chemical modification of membrane proteins in relation to inhibition of anion exchange in human red blood cells. *J. Cell. Physiol.*, **86**:471 (3)